applied sciences

MDPI

Article

Advanced Unified Earthquake Catalog for North East India

Pallavi [1], Ranjit Das [2,*], Sandeep Joshi [1], Claudio Meneses [2] and Tinku Biswas [3]

[1] School of Computing and IT, Manipal University Jaipur, Jaipur 303007, India
[2] Computer Science Department, Universidad Catolica del Norte, Antofagasta 1249004, Chile
[3] Earthquake Engineering Department, Indian Institute of Technology Roorkee, Roorkee 247667, India
* Correspondence: ranjit.das@ucn.cl

Abstract: Northeast India is one of the world's most seismically active regions. The event data included in this research for the period 1737–2012 is mostly obtained from worldwide database agencies such as ISC, NEIC, and GCMT. Historical seismicity is collected from published and unpublished documents and some earthquake events are collected from the Indian Meteorological Department Bulletins. As the M_w scale is developed and validated in the southern California region and overestimates the smaller magnitude earthquakes, therefore, recent literature suggested an improved version of the seismic moment magnitude scale (M_{wg}) applicable for the entire globe considering both long- and short-period frequency-spectra using modern instrumental data. To update the earthquake catalog of Northeast India, we prepared empirical relationships between different magnitudes to M_{wg} using robust statistical General Orthogonal Regression. A procedure is also suggested for converting different earthquake sizes towards seismic moment scale. The Magnitude of Completeness (M_c) and the Gutenberg–Richter (GR) recurrence parameter values for the declustered homogenized catalog in four time periods, namely 1737–1963, 1964–1990, 1964–2000, and 1964–2012, have been computed. Our analysis suggests that the use of the M_{wg} scale improves seismicity parameters 'b' up to 30%, 'a' up to 17%, and 'M_c' up to 18% for the Northeast India region. A complete unified earthquake catalog in terms of advanced seismic moment magnitude scale could help understand seismicity and earthquake engineering studies of the region.

Keywords: homogenous earthquake catalog; North East region; general orthogonal regression; seismogenic zones

Citation: P.; Das, R.; Joshi, S.; Meneses, C.; Biswas, T. Advanced Unified Earthquake Catalog for North East India. *Appl. Sci.* **2023**, *13*, 2812. https://doi.org/10.3390/app13052812

Academic Editors: Wei-Ling Hsu, Yan-Chyuan Shiau and Hsin-Lung Liu

Received: 19 December 2022
Revised: 15 January 2023
Accepted: 24 January 2023
Published: 22 February 2023

1. Introduction

Earthquakes are inherently complex phenomena, and because of differences in equipment characteristics and station coverage used to record seismic waves at different epicentral distances, most magnitude estimations in space and time are subject to measurement errors. Several earthquake magnitude scales have been used in seismic catalogs to represent the earthquake size, such as M_L (Local Magnitude), m_b (Body Wave Magnitude), M_s (Surface Wave Magnitude), and M_w (Moment Magnitude). Recent studies (e.g., [1–5]) show that the M_w scale has some serious drawbacks in representing earthquake size. Many authors stated that the M_w scale is not suitable for frequencies applicable for engineering importance (e.g., [3,6,7]). The M_w scale underestimates large earthquakes such as the 11 March 2011—Tohoku-Oki earthquake and the 26 December 2004—Sumatra earthquakes (e.g., [1,3–5]) and overestimates the smaller earthquakes (e.g., [1]). Although the M_w scale is expressed in terms of the moment (Mo), however, it is mainly based on surface waves; therefore, it is not a good representation of the seismic source. As the philosophy of the M_w scale [8] is based on surface waves and, therefore, it is inappropriate for deeper earthquakes. Furthermore, the M_w scale is mainly derived and validated based on Southern California tectonics [8]. The M_w scale given by Ref. [8] is valid for global earthquakes in the magnitude range >7.5 because the M_w scale is based on bigger magnitude earthquakes at the global level. As the seismic moment is mainly derived from surface waves (e.g., [9]),

the formulation of the M_w scale (i.e., ´2/3' and '10.7') also originated from surface wave magnitude. Thus, the M_w scale relates to long-period seismic spectra. Furthermore, the M_w scale was developed based on constant value for tectonic effect for shallow earthquakes. There was no statistical validation while developing the M_w scale, only a comparison of the M_w scale with some Southern Californian earthquakes [8]. Ref. [1] provide a magnitude scale mainly considering global tectonics. As the M_{wg} scale is developed by considering p-wave along with consideration of seismic moment M_0, and M_0 is computed from the surface wave trend of the seismic signal ([9,10]). Thus, the M_{wg} scale covers both high and low-frequency spectra of the seismic signal. The M_{wg} scale is preferable to the M_w scale mainly for the following reasons: (1) the M_w scales underestimate the bigger earthquake and overestimate the smaller and intermediate earthquakes (e.g., [1,5]); (2) the M_{wg} scale is based on directly observed M_o whereas the M_w formulation in terms of M_0 was not derived based on observed M_0 but rather based on substitution assuming constant values; (3) In the case of M_{wg}, the proper representation of global seismicity has been considered for minor, moderate, and large earthquakes, and on the other hand, M_w is based on the seismicity of Southern California, particularly for minor and intermediate occurrences; (4) M_w is not a good estimate for high-frequency ground motions, which are critical for estimating the potential shaking damage of earthquakes as M_w is defined from very long period spectral amplitudes. M_{wg}, on the other hand, is calculated from low- and high-frequency seismic spectra and thus fills the gap left by M_w.

Uncertainties associated with distinct magnitude scales play a significant role during magnitude conversions into a single magnitude scale. Regression relationships are used to transform diverse magnitudes into seismic moment scales to construct a homogeneous earthquake database (M_{wg}). General orthogonal regression (GOR) methodology is better suited for homogenizing seismicity catalogs to create regression relationships between distinct magnitude classes [11–19]. Various scaling relationships have been developed to homogenize an earthquake database for Northeast India [5,11,13–24]. Ref. [11] used GOR to convert body and surface wave magnitude scales into M_w, and substantial dispersion was found in the translation of $m_{b,ISC}$ into M_w. Ref. [21] made the conversion of m_b and M_s into M_w using the least-square regression (SLR) approach. Refs. [13,14] performed regression analysis for m_b to M_w and M_s to M_w using SLR, GOR, and inverted standard regression (ISR). Ref. [5] recently developed empirical relationships between different magnitudes into M_w using an improved version of the GOR technique (GOR1). Still date, the developed empirical relationships are in terms of M_w for the Northeast India region. This is the first study that gives a homogenous earthquake database for the Northeast India region using an improved magnitude scale. An enhanced GOR approach (GOR1) is applied in this investigation, as detailed in Ref. [20], for establishing regression relationships from different magnitudes to M_{wg} on a regional basis. For the period 1737–2012, a dataset of 9968 earthquake occurrences in the magnitude range 1.6–8.7 corresponding to the study area (lat. 20–30° and long. 87–98°) is employed. GOR relationships for conversion of m_b and M_s into M_{wg} are developed using regional datasets. The prepared homogenous catalog will be useful not only for seismic risk assessment but also for other seismological applications. Following the unification of the earthquake catalog towards seismic moment magnitude scale M_{wg}, declustering has been performed, and its completeness is assessed in the sections that follow.

2. Seismicity of North East India

Figure 1 displays a seismotectonic map indicating the epicenters of $M_{wg} \geq 2$ occurrences from 1737 to 2012, as well as the geological aspects of the NE India region ranging from 20–30° N latitude to 87–98° E longitude. The Shillong earthquake of 12 June 1897 (M_{wg} = 8.9) and the Assam earthquake of 15 August 1950 (M_{wg} = 8.6) are the two recent big earthquakes in this area. Furthermore, a succession of significant earthquakes ($M_{wg} \geq 7.0$) has occurred in this area, resulting in the loss of lives and the damage of property. Ref. [25] classified the area into four primary seismogenic root zones: the Eastern Syntax (zone I), the

Arakan–Yoma Subduction Belt (zone II), the Shillong Plateau (zone III), and the Himalayan Frontal Thrusts Main Central Thrust (MCT) and Main Boundary Thrust (MBT) (zone IV). Seismicity in this region is caused by the collision of the Indian Plate and Tibet in the north and the Burmese landmass in the east. As a result of such collisions, the Himalayan Thrust system was formed in the north, the Arakan–Yoma Mountain Arc, the Naga Hills, the Tripura Folded Belt in the east, and the Shillong Plateau rose.

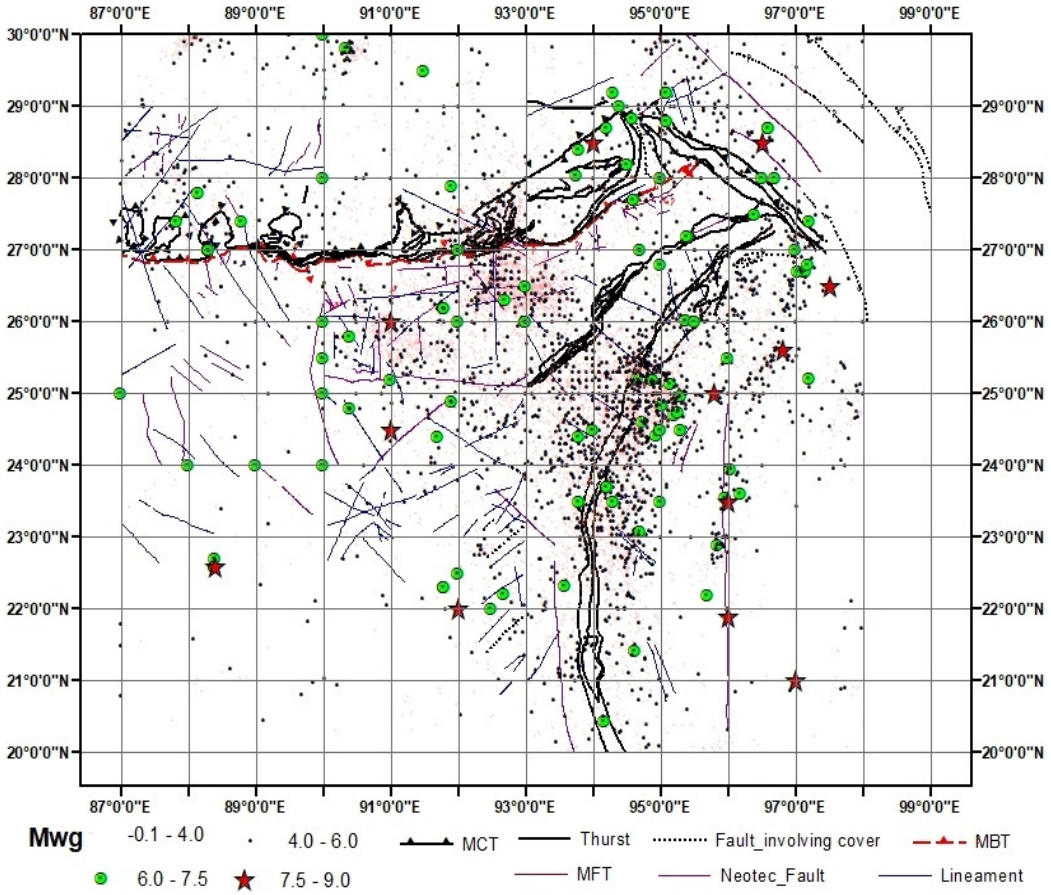

Figure 1. Seismotectonic map exhibiting seismicity for $M_{wg} \geq 2$ with epicenters and tectonic characteristics of the NE India region on a GIS platform.

The Shillong massif stands out as a plateau with an average elevation of 1500 m near the basin's SW outlet. The seismic zones of Ref. [25] are further classified into nine seismogenic zones, as illustrated in Table 1 and Figure 2 [20]. The subdivision focuses on tectonic and geological faults, focal mechanism solutions, and the geographical distribution of earthquake events [20].

Table 1. Different Seismogenic zones for Northeast India.

Seismogenic Zone	Major Division	Subdivision
I	Indo Burma Fault Belt	NS Indo-Burma Fold Belt
II	Indo Burma Fault Belt	NE-SW Indo Burma Fold Belt
III	Plateau Region	Sagging Fault Region
IV	Mishmi Massif	NW-SE trending feature
V	Plateau Region	Tibetan Plateau
VI	Himalayan Mountain Belt	Eastern MCT

Table 1. *Cont.*

Seismogenic Zone	Major Division	Subdivision
VII	Shillong Massif	Shillong Plateau
VIII	Bengal Basin	Sylhet Fault
IX	Himalayan Mountain Belt	NE-SW trending Structure

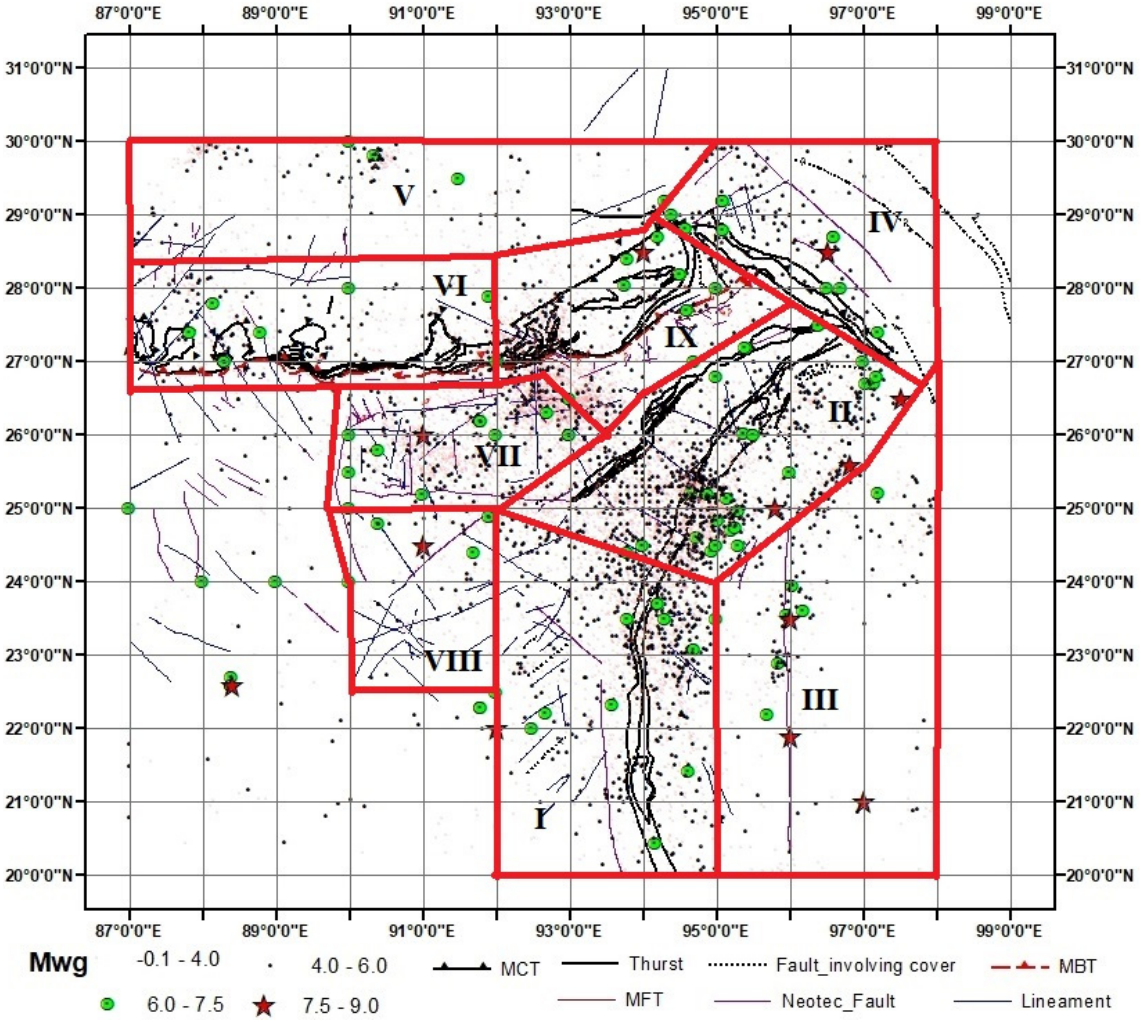

Figure 2. Seismogenic source zones (I-IX) are being considered for Northeast India.

3. Data

The body and surface wave magnitudes are considered by ISC (International Seismological Center; UK, http://www.isc.ac.uk/search/Bulletin (last accessed on 18 August 2012)), and the seismic moment is considered with GCMT (Global Centroid Moment Tensor database http://www.globalcmt.org/CMTsearch.html (last accessed on 18 October 2012)). Data of 9968 earthquake events from 1737 to 2012 are obtained from several sources for the examined region (e.g., ISC, NEIC, GCMT, IMD: Indian Meteorological Department). For historical seismicity from 1897 to 1962, data are obtained from Ref. [26].

4. Regression Analysis for Magnitude Conversion

General Orthogonal Regression (GOR) is a method for establishing a connection between two variables in which measurement errors for both variables are considered. The method for carrying out the GOR is defined by many authors [13,16,18,27–30] and is not included here. A detailed description has been given in Appendix A.

The GOR equation is in the form of $M_Y = \beta_0 + \beta_1 M_x$ but has been used in a different form $M_Y = \beta_0 + \beta_1 m_x$ and this practice is referred to as GOR2 (see Appendix A; various notations used in GOR methodology are explained in Appendix B). Note that $M_x \neq m_x, M_x$ is the theoretical true point on the GOR line and m_x is the observed data point. Replacing m_x in place of M_x in the GOR relation leads to biased estimates of the dependent variable. Many investigators pointed out the limitations of GOR2, Ref. [19] stated that GOR2 provides overestimated slope as an error variance ratio ($\eta = \frac{\sigma_\varepsilon^2}{\sigma_\delta^2}$) does not encounter equation errors. Ref. [19] provided a method for encountering equation error and minimization of overestimation of slope for the GOR2 methodology. Ref. [19] proved theoretically and synthetically that GOR1 provides better estimates than GOR2 and SLR (Standard Least Squared Regression). GOR1 provides the highest accuracy in dependent variable estimations as compared to the conventional GOR2 and SLR approaches. Given all these reasons, we are using GOR1 for our analysis.

4.1. Surface Wave and Body Wave Conversions

The GOR1 methodology has been used to convert magnitudes such as M_s and m_b to $M_{wg,GCMT}$. The GOR1 relationship for $M_{s,ISC}$ to $M_{wg,GCMT}$ has been developed in the range $4.1 \leq M_{s,ISC} \leq 6.1$, using 93 case data and assuming $\eta = 0.6$, is obtained as follows:

$$M_{wg,GCMT} = 0.680(\pm 0.002)\, M_{s,ISC} + 1.69(\pm 0.08). \quad (1)$$

$$R_{xy} = 0.94, \quad RMSE = 0.094, \quad n = 93$$

The regression plot for $M_{s,ISC}$ to $M_{wg,GCMT}$ has been shown in Figure 3. The above obtained GOR1 relationship is found with the lowest error values in terms of slope, intercept, standard deviation, and root means square error as compared to SLR and GOR2 (Tables 2 and 3, Figure 4). The correlation coefficient value (R_{xy}) obtained using the GOR1 methodology shows significant improvement as compared to GOR2 and SLR (Tables 2 and 3). The maximum difference between M_{wg} estimation using $M_{s,ISC}$, and the corresponding M_w estimation of Ref. [5] is found to be 0.4.

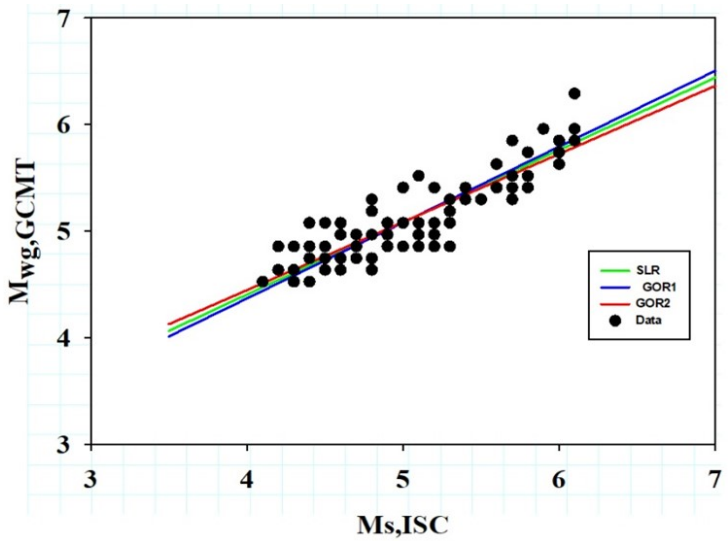

Figure 3. The ($M_{S,ISC}$ − Mwg) data, as well as the GOR1, GOR2, and SLR regression lines.

Table 2. Comparisons of regression parameters of GOR1, GOR2 and SLR for Northeast India Region Datasets.

Regression Relation	Magnitude Range	Slope (GOR1)	Intercept (GOR1)	Slope (GOR2)	Intercept (GOR2)	Slope SLR	Intercept SLR	R_{xy} GOR1	R_{xy} GOR2	R_{xy} SLR	RMSE GOR1	RMSE GOR2	RMSE SLR
$m_{b,\ ISC}$ to M_{wg} $\eta = 0.2$	$4.8 \leq m_{b,\ ISC} \leq 6.1$	1.19	−1.19	1.61	−3.38	1.16	−1.01	0.74	0.59	0.69	0.22	0.28	0.24
$m_{b,\ NEIC}$ to M_{wg} $\eta = 0.2$	$4.8 \leq m_{b,\ NEIC} \leq 6.1$	1.21	−1.39	1.68	−3.89	1.18	−1.27	0.72	0.55	0.68	0.2	0.26	0.22
$M_{s,ISC}$ to $M_{wg}\eta = 0.6$	$4.1 \leq M_{s,\ ISC} \leq 6.1$	0.68	1.69	0.71	1.525	0.64	1.89	0.97	0.88	0.9	0.08	0.19	0.18
$M_{s,NEIC}$ to $M_{wg}\eta = 0.6$	$4.2 \leq M_{s,\ NEIC} \leq 6.1$	0.77	1.19	0.82	0.97	0.73	1.40	0.94	0.79	0.8	0.09	0.18	0.17
Intensity to M_{wg} $\eta = 1$	5 to 12	0.48	3.07	0.49	3.00	0.44	3.36	0.98	0.61	0.62	0.13	0.69	0.68
Local Magnitude $\eta = 1$	$5.0 \leq M_L \leq 6.6$	1.31	−1.89	1.47	−2.76	1.24	−1.49	0.89	0.74	0.77	0.16	0.25	0.24
Duration Magnitude $\eta = 1$	$4.2 \leq M_D \leq 6.8$	0.82	0.83	1.007	−0.109	0.64	1.76	0.81	0.26	0.4	0.14	0.3	0.27

Table 3. The list of error metrics for regression parameters such as Error in Slope, Error in intercept, Mean Square Error, Mean Average Error, and Root Mean square Error corresponding to the derived regression relations for this study [16,31].

Regression Relation	Magnitude Range	Error in Slope			Error in Intercept			MSE			MAE			RMSE		
		GOR1	GOR2	SLR	GOR1	GOR2	SLR	GOR1	GOR2	SLR	GOR1	GOR2	SLR	GOR1	GOR2	SLR
$m_{b,\ ISC}$ to M_{wg} η=0.2	$4.8 \leq m_{b,\ ISC} \leq 6.1$	±0.01	±0.098	±0.07	± 0.35	±0.49	± 0.37	0.049	0.07	0.06	0.17	0.22	0.19	0.22	0.28	0.24
$m_{b,\ NEIC}$ to M_{wg} η=0.2	$4.8 \leq m_{b,\ NEIC} \leq 6.1$	±0.02	±0.11	±0.08	± 0.37	±0.60	± 0.42	0.04	0.29	0.05	0.17	0.47	0.19	0.2	0.26	0.22
$M_{s,ISC}$ to M_{wg} η=0.6	$4.1 \leq M_{s,\ ISC} \leq 6.1$	±0.00	±0.04	±0.03	±0.08	±0.24	± 0.18	0.01	0.04	0.04	0.07	0.16	0.15	0.08	0.19	0.18
$M_{s,NEIC}$ to M_{wg} η=0.6	$4.2 \leq M_{s,\ NEIC} \leq 6.1$	±0.00	±0.05	±0.05	±0.13	±0.326	± 0.23	0.01	0.03	0.03	0.07	0.15	0.14	0.09	0.18	0.17
Intensity to M_{wg} η=1	5 to 12	±0.001	±0.07	±0.07	±0.51	±1.38	± 0.50	0.02	0.44	0.43	0.1	0.53	0.52	0.13	0.69	0.68
Local Magnitude η=1	$5.0 \leq M_L \leq 6.6$	±0.00	±0.08	±0.07	±0.25	±0.5	± 0.37	0.02	0.06	0.56	0.02	0.11	0.02	0.16	0.25	0.24
Duration Magnitude η=1	$4.2 \leq M_D \leq 6.8$	±0.002	±0.06	±0.04	±0.10213	±0.35774	± 0.203	0.01	0.05	0.05	0.11	0.31	0.22	0.14	0.3	0.27

Similarly, to convert $M_{s,NEIC}$ to $M_{wg,GCMT}$, we are taking into account 57 earthquake events in the range $4.2 \leq M_{s,NEIC} \leq 6.1$, and the GOR1 relationship is shown below.

$$M_{wg,GCMT} = 0.771(\pm 0.003)M_{S,NEIC} + 1.193(\pm 0.126). \quad (2)$$

$$R_{xy} = 0.94, \quad RMSE = 0.092, \quad n = 57$$

The regression plots for the relationships between $M_{s,NEIC}$, and M_{wg} are shown in Figure 5. We observed GOR1 methodology for conversion of $M_{s,NEIC}$ towards M_{wg} shows significant improvement in terms of error of slope, intercept, RMSE and R_{xy} as compared to the other two methods (Tables 2 and 3 and Figure 6).

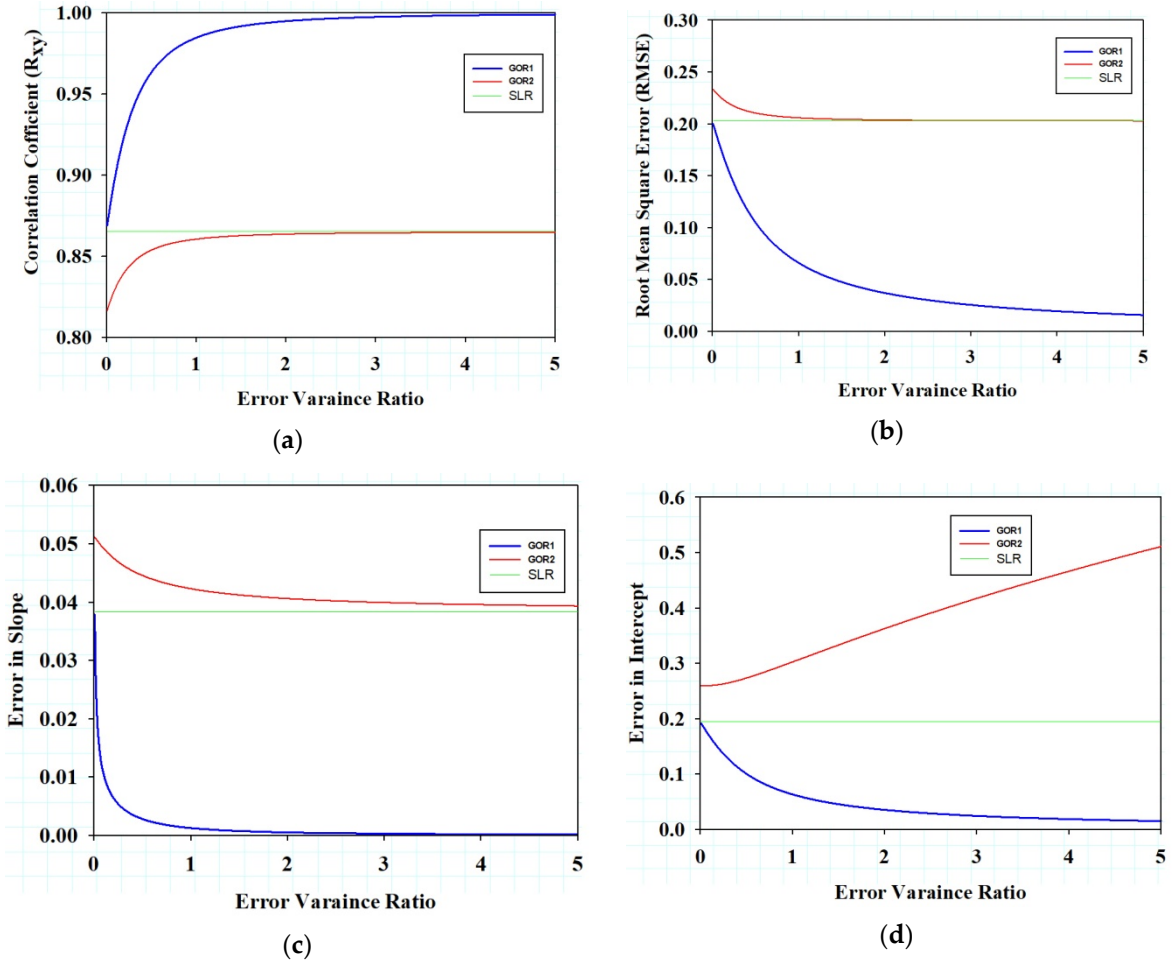

Figure 4. Comparison of the uncertainty in regression parameters for ($M_{S,ISC} - M_{wg}$) data pairs using GOR1, GOR2, and SLR approaches considering function of error variance ratio: (**a**) Correlation Coefficient determination (R_{xy}), (**b**) Root mean square error (RMSE), (**c**) uncertainty values of slope and (**d**) uncertainty of intercept.

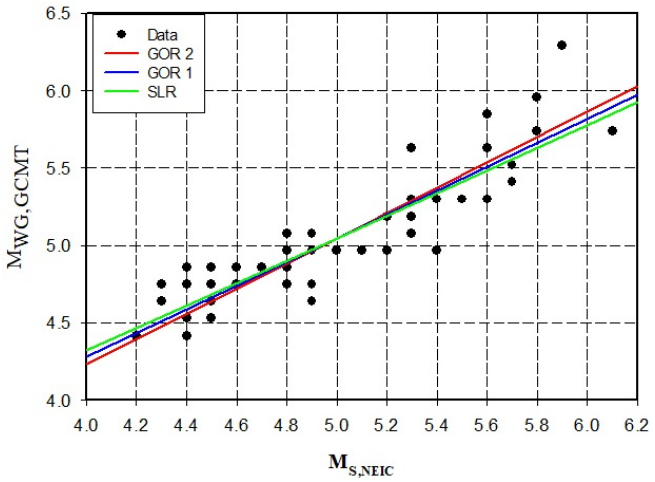

Figure 5. The ($M_{S,NEIC} - M_{wg}$) data, as well as the GOR1, GOR2, and SLR regression lines.

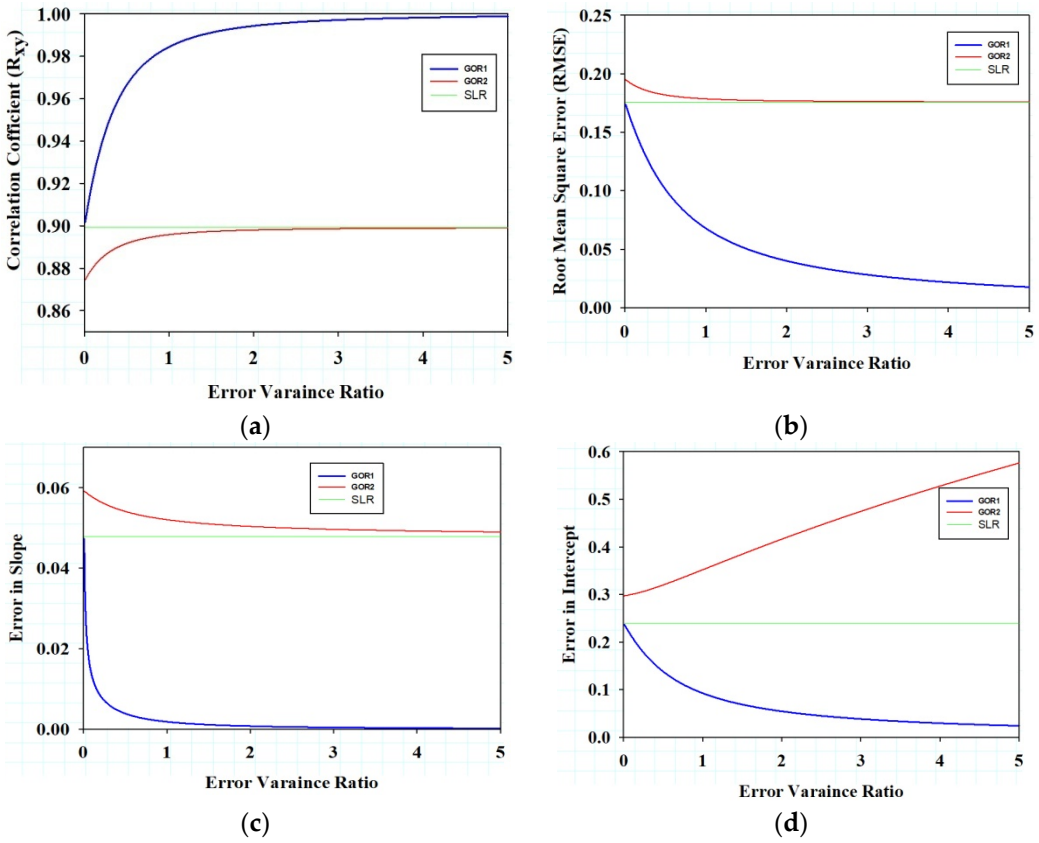

Figure 6. Comparison of the uncertainty in regression parameters for ($M_{S,NEIC}$ – M_{wg}) data pairs using GOR1, GOR2, and SLR approaches considering function of error variance ratio: (**a**) Correlation Coefficient determination (R_{xy}), (**b**) Root mean square error (RMSE), (**c**) uncertainty values of slope and (**d**) uncertainty of intercept.

For changeover of $m_{b,ISC}$ to $M_{wg,GCMT}$ for magnitude range $4.8 \leq m_{b,ISC} \leq 6.1$, and $m_{b,NEIC}$ to $M_{wg,GCMT}$ for magnitude range $4.8 \leq m_{b,NEIC} \leq 6.1$, the same methodology has been adopted by datasets of 116 and 106 for the period 1964–2012, respectively. The GOR1 relationship between $M_{wg,GCMT,}$ and $m_{b,ISC}$ is obtained using $\eta = 0.2$ and is given below. The regression plot is shown in Figure 7.

$$M_{wg,GCMT} = 1.19(\pm 0.014)m_{b,ISC} - 1.190(\pm 0.347). \quad (3)$$

$$R_{xy} = 0.74, \quad RMSE = 0.224, \quad n = 116.$$

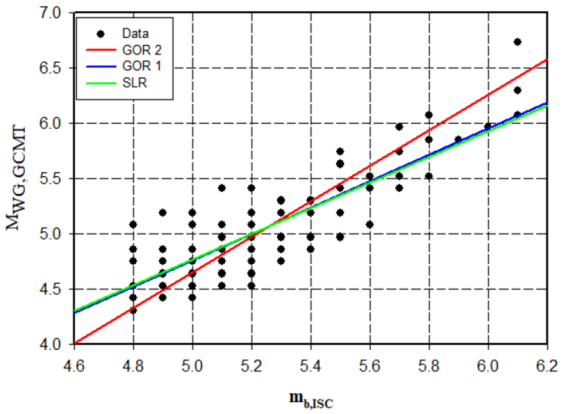

Figure 7. The ($m_{b,ISC}$ − M_{wg}) data, as well as the GOR1, GOR2, and SLR regression lines.

The maximum difference between M_{wg} (using Equation (3)) and M_w (using the corresponding equation of Ref. [5]) is found to be 0.4. The GOR1 methodology for conversion of $m_{b,ISC}$ to M_{wg} shows lower errors in slope and intercept as compared to SLR and GOR2. The GOR1 method provides significant improvement in the correlation coefficient (R_{xy}) and standard error (RMSE) as compared to GOR2 and SLR approaches (Tables 2 and 3 and Figure 8).

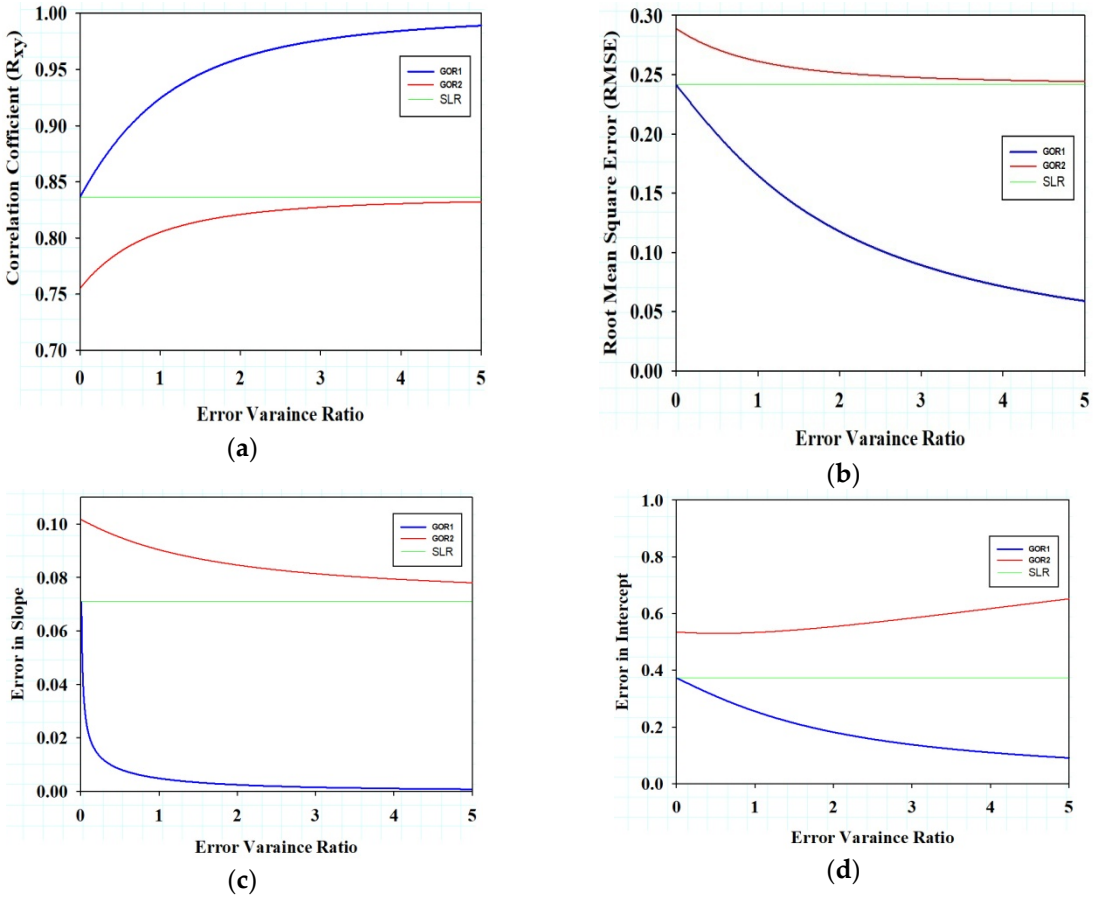

Figure 8. Comparison of the uncertainty in regression parameters for ($m_{b,ISC} - M_{wg}$) data pairs using GOR1, GOR2, and SLR approaches considering the function of error variance ratio: (**a**) Correlation Coefficient determination (R_{xy}), (**b**) Root mean square error (RMSE), (**c**) uncertainty values of slope and (**d**) uncertainty of intercept.

The relationship between $m_{b,NEIC,}$ and M_{wg} with η equal to 0.2 is stated as

$$M_{wg,GCMT} = 1.21(\pm 0.016)m_{b,NEIC} - 1.391(\pm 0.390). \quad (4)$$

$$R_{xy} = 0.72, \quad RMSE = 0.201, \quad n = 106.$$

The regression plot for $m_{b,NEIC}$ to $M_{wg,GCMT}$ has been shown in Figure 9. The difference between M_{wg} estimation using Equation (8) and the corresponding M_w of Ref. [5] is found to be 0.4. Furthermore, the GOR1 methodology shows significant improvement in lowering errors of slope and intercept (Tables 2 and 3 and Figure 10). GOR1 methodology also shows improvement in R_{xy} and RMSE values (Tables 2 and 3 and Figure 10) for conversion of $m_{b,NEIC}$ to M_{wg}.

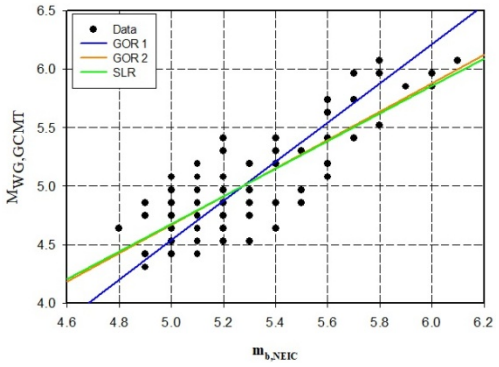

Figure 9. The ($m_{b,NEIC}$ − M_{wg}) data, as well as the GOR1, GOR2, and SLR regression lines.

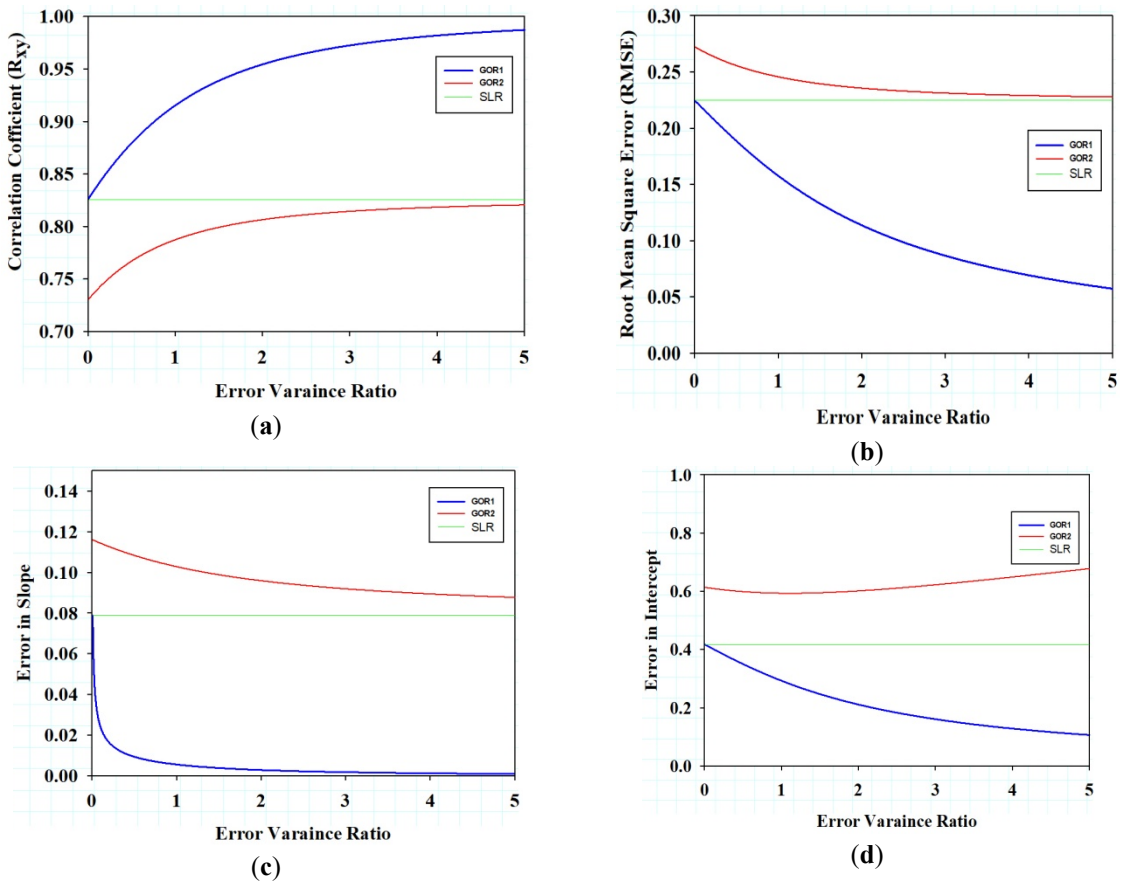

Figure 10. Comparison of the uncertainty in regression parameters for ($m_{b,NEIC}$ − M_{wg}) data pairs using GOR1, GOR2, and SLR approaches considering function of error variance ratio: (**a**) Correlation Coefficient determination (R_{xy}), (**b**) Root mean square error (RMSE), (**c**) uncertainty values of slope and (**d**) uncertainty of intercept.

4.2. Local Magnitude into M_{wg}

For the period 1976–2005, the relationship between local magnitude and seismic moment magnitude is determined using 100 earthquakes in Northeast India. The derived GOR1 relationship using η = 1 is given below. The required plot for the corresponding relationship is shown in Figure 11:

$$M_{wg,GCMT} = 1.31\ (\pm 0.005)\ M_L - 1.890\ (\pm 0.25),\ 5 \leq M_L \leq 6.6 \quad (5)$$

$$R_{xy} = 0.89, \quad RMSE = 0.164, \quad n = 100.$$

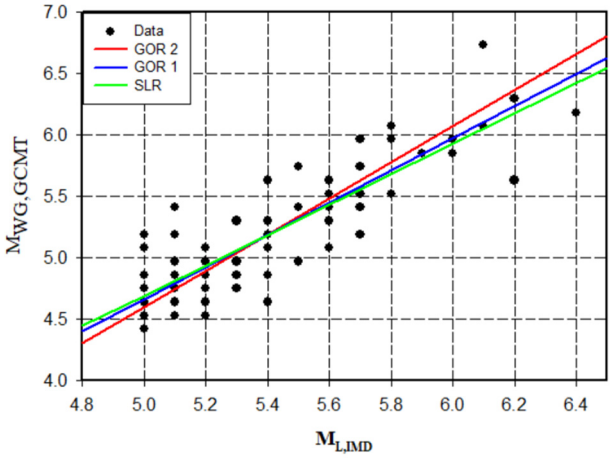

Figure 11. The ($M_L - M_{wg}$) data, as well as the GOR1, GOR2, and SLR regression lines.

The maximum difference between Mw estimations from Ref. [5] and M_{wg} estimations in the present study for local magnitude conversion is found to be 0.3. This difference can be higher than 0.3 while considering a larger magnitude range. The GOR1 relationship for M_L to M_{wg} has the highest accuracy in terms of the uncertainty of the regression coefficients when compared to SLR and GOR2 (Figure 12 and Tables 2 and 3).

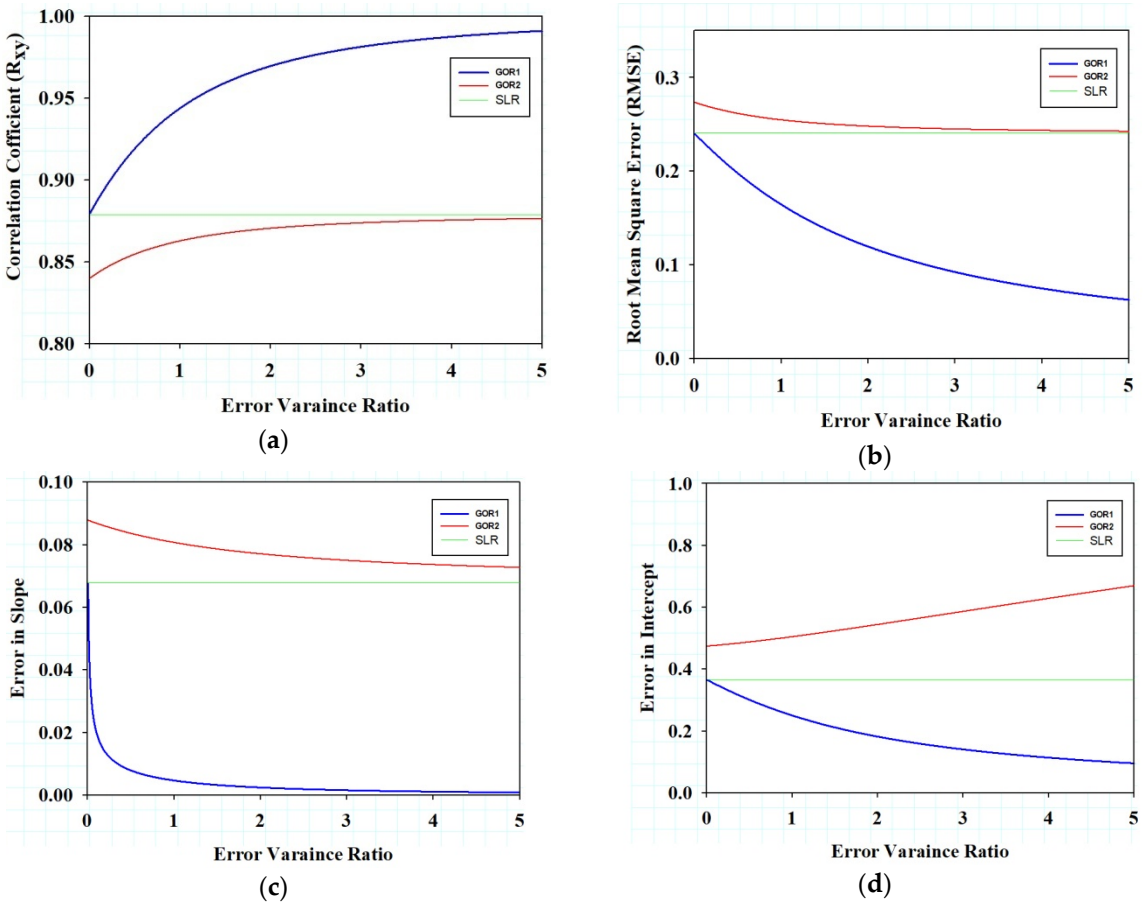

Figure 12. Comparison of the uncertainty in regression parameters for ($M_L - M_{wg}$) data pairs using GOR1, GOR2, and SLR approaches considering function of error variance ratio: (**a**) Correlation Coefficient determination (R_{xy}), (**b**) Root mean square error (RMSE), (**c**) uncertainty values of slope and (**d**) uncertainty of intercept.

4.3. Duration Magnitudes into M_{wg}

Based on 376 global data earthquakes from the ISC database, the relationship between duration magnitude (M_D) and M_{wg} is derived using GOR1 methodology with $\eta = 1$ and is given below. The plot of the regression is shown in Figure 13.

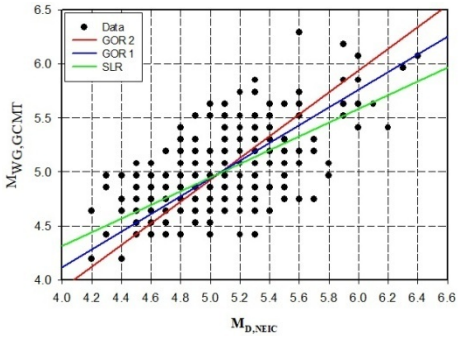

Figure 13. The ($M_D - M_{wg}$) data, as well as the GOR1, GOR2, and SLR regression lines.

The relationship between M_D and M_{wg} using $\eta = 1$ is stated as

$$M_{wg,GCMT} = 0.821(\pm 0.002)M_D - 0.832(\pm 0.102). \quad (6)$$

$$R_{xy} = 0.81, \quad RMSE = 0.140, \quad n = 376.$$

For the conversion of M_D to M_{wg}, it is also found that the GOR1 method has the highest accuracy compared to SLR and GOR2 (Tables 2 and 3 and Figure 14).

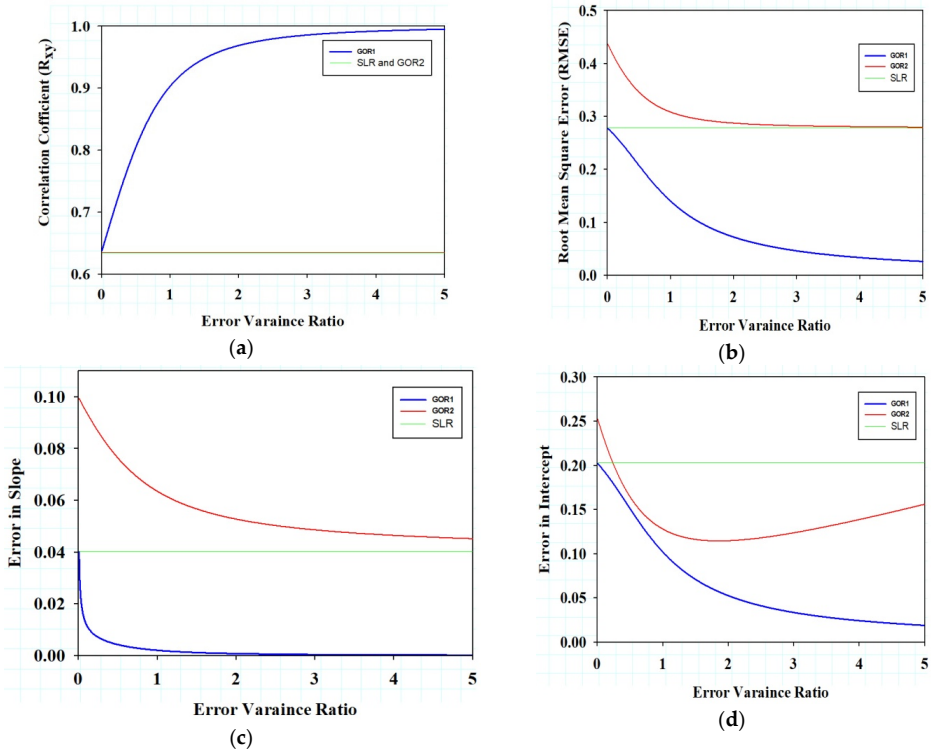

Figure 14. Comparison of the uncertainty in regression parameters for ($M_D - M_{wg}$) data pairs using GOR1, GOR2, and SLR approaches considering function of error variance ratio: (**a**) Correlation Coefficient determination (R_{xy}), (**b**) Root mean square error (RMSE), (**c**) uncertainty values of slope and (**d**) uncertainty of intercept.

4.4. Intensity Conversion Relation

Considering 29 earthquakes in India and adjacent areas from 1897 to 2016, a magnitude–intensity GOR1 relationship has been developed, with independent MMI (I_0) in the range 5–12 and seismic moment magnitude (M_{wg}) determined from several sources, as follows:

$$M_{wg,GCMT} = 0.48\ I_{max} + 3.07(0.1) \quad (7)$$

Figure 15 depicts the plot of the Intensity relationship.

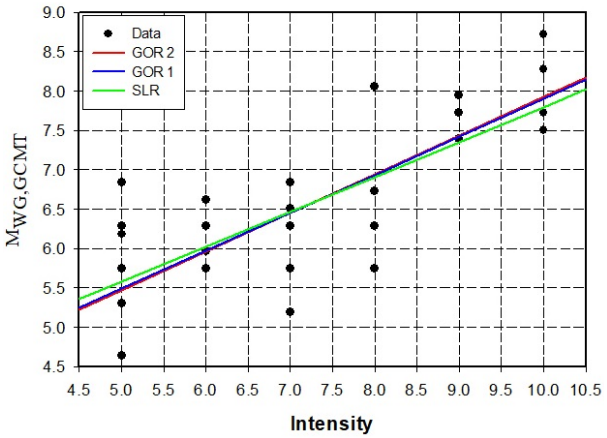

Figure 15. Plot showing the GOR connection for intensity scaling (MMI) to $M_{wg,GCMT}$.

Ref. [5] derived the GOR1 relationships between M_w and MMI for the same datasets and found a lower slope (0.389) than the present study (0.48). The maximum difference between M_w and M_{wg} estimations using MMI is found to be 0.5, which may lead to serious biased in the preparation of seismicity parameters. It is found that the GOR1 relationship derived between MMI and M_{wg} has the highest accuracy when compared to SLR and GOR2 (Tables 2 and 3).

The GOR1 relationships derived above for the study region are compared to the similar GOR1 relationships derived by Ref. [5] for NE India and its bordering region. It is found that the regression relationships derived in this work for the NE India area are not the same as those defined by Ref. [5], as in this paper, the regression relationship is for the seismic moment magnitude (M_{wg}) while Ref. [5] is for the moment magnitude (M_w). For easy reference to the reader, we are reproducing the GOR1 relationships of Ref. [5] as below:

$$M_{w,GCMT} = 0.615\ M_{s,ISC} + 2.32,\ 4.1 \leq M_{s,ISC} \leq 6.1 \quad (8)$$

$$M_{w,GCMT} = 0.699\ M_{s,NEIC} + 1.878,\ 4.2 \leq M_{s,NEIC} \leq 6.1 \quad (9)$$

$$M_{w,GCMT} = 1.084\ m_{b,ISC} - 0.3106,\ 4.8 \leq m_{b,ISC} \leq 6 \quad (10)$$

$$M_{w,GCMT} = 1.104 m_{b,NEIC} - 0.495,\ 4.8 \leq m_{b,NEIC} \leq 6.1 \quad (11)$$

$$M_{w,GCMT} = 1.193 M_L - 0.943,\ 5.0 \leq M_L \leq 6.6 \quad (12)$$

$$M_{w,GCMT} = 0.742 M_D + 1.565,\ 4.2 \leq M_D \leq 6.8 \quad (13)$$

Appendix B contains abbreviations for various magnitude scales. A procedure for conversion of different magnitudes towards seismic moment scale M_{wg} has been suggested in Appendix C. Homogeneous earthquake catalog in terms of M_{wg} has been reported in Appendix A. A full data catalog can be obtained from the corresponding author.

5. Declustering of the Catalog

In general, the earthquake catalog is composed of foreshocks, mainshocks, and aftershocks Ref. [32]. Foreshocks and aftershocks should be excluded from the catalog for the

evaluation of seismic hazards because they are dependent events. Several strategies for declustering a catalog have been proposed (e.g., [33–36]). We use a space and time window technique of Ref. [36] procedure for declustering the catalog (Figure 16). After declustering, there are 942 earthquake clusters, a total of 2231 (22.381%) occurrences eliminated from the homogenized catalog of 9968 events using the GOR1 method for the period 1737–2012. The seismic moment released by the clusters is about 3.7554% of the total seismic moment of the catalog.

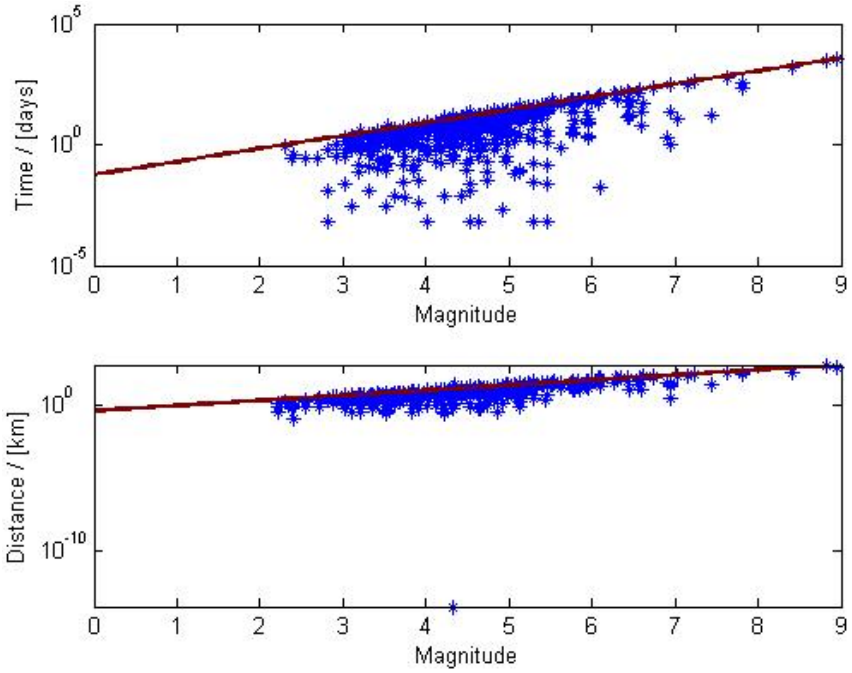

Figure 16. Aftershocks are removed using magnitude-dependent spatial and temporal frames (dependent occurrences). The asterisks under the window lines are interpreted as dependent occurrences.

After declustering of the homogenized catalog of M_w in Ref. [5], there are 1232 earthquake clusters, a total of 3178 (31.882%) occurrences eliminated from the total catalog of 9968 earthquake events for the period 1737–2012. The seismic moment released by the clusters is about 14.313% of the total seismic moment of the catalog. Thus, we can see that the number of clusters in M_w is more than in M_{wg}.

6. The Magnitude of Completeness (M_c)

Declustered earthquake catalogs for the periods 1737–1963, 1964–1990, 1964–2000, and 1964–2012 have been studied to distinguish temporal differences in earthquake happenings in NE India. Four graphs, corresponding to four different periods, have been plotted to show the relationships between various bin of magnitudes and the corresponding cumulative number of events having an earthquake magnitude greater than the corresponding magnitude of completeness (Figure 17).

The Magnitude of Completeness M_c has been calculated by the EMR method [37] for various catalog times using the ZMAP program. M_c values are seen to decline with the introduction of the newest information throughout time (Table 4). As the detection threshold for the sample area increased from 1964 onwards, the general trend of the 'b' value continuously decreased over time, resulting in the recording of a greater number of smaller magnitude earthquakes in proportion to large magnitude occurrences, as seen in Table 4.

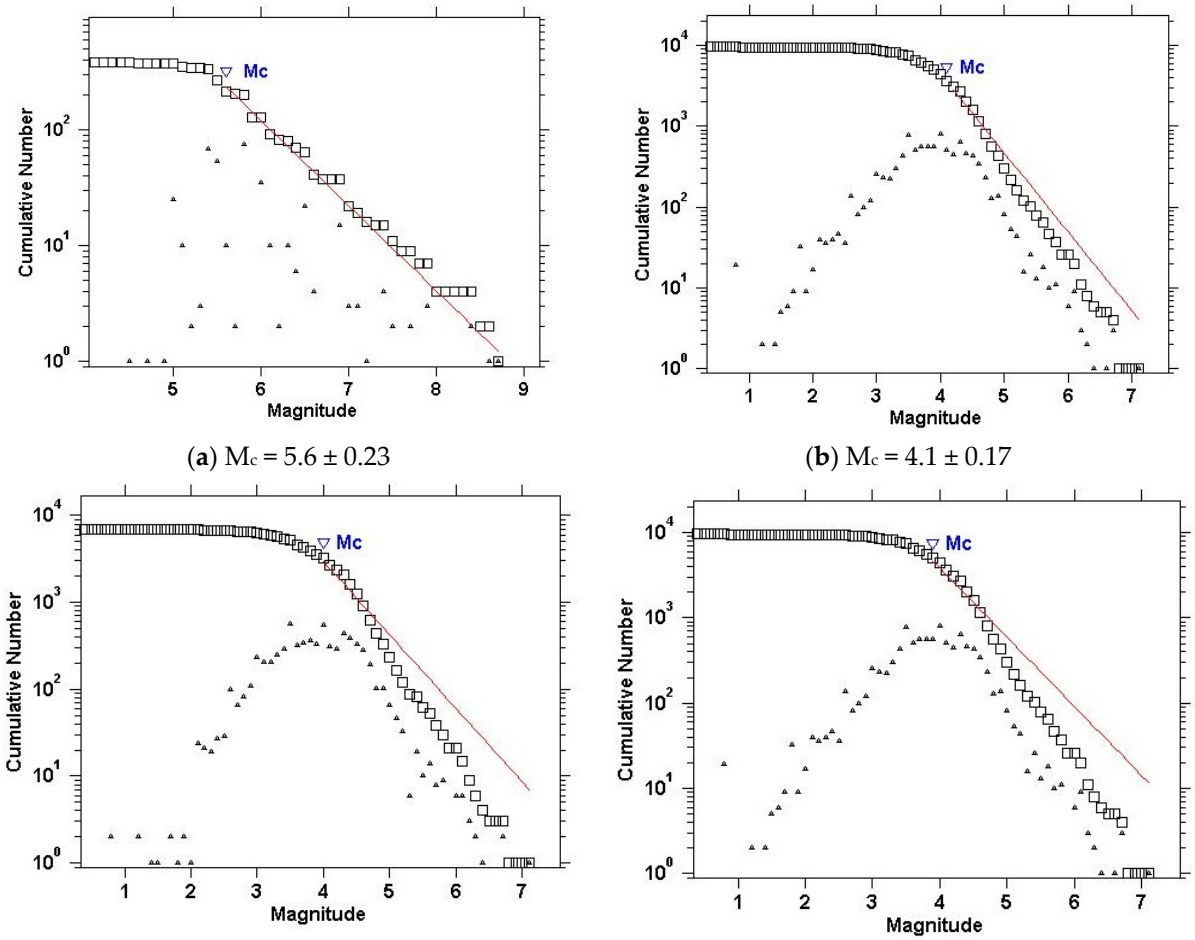

Figure 17. Four different plots showing the cumulative number of earthquake events vs. magnitudes greater than the corresponding magnitude for the following catalog time periods (**a**) 1737–1963, (**b**) 1964–1990, (**c**) 1964–2000, and (**d**) 1964–2012. In addition, these plots show M_c values determined by the EMR technique.

Table 4. Estimated Mc, 'b,' and 'a' values for various catalogs.

Catalog Time Periods	M_c	b	a
1737–1963	5.6 ± 0.23	0.74	6.5
1964–1990	4.1 ± 0.17	0.98	7.56
1964–2000	4 ± 0.17	0.85	6.86
1964–2012	3.9 ± 0.23	0.81	6.83

In the M_w catalog, the EMR approach is used to determine M_c for various catalog time periods using the ZMAP application. M_c values are decreasing w.r.t increasing time periods. From 1964 onwards, the detection threshold for the sample region is constantly grown over time, resulting in the recording of a higher number of lower magnitude earthquakes to big magnitude events. The value of M_c for the M_w catalog is more than the M_{wg} catalog (Table 5). This shows that more earthquakes within a certain region are more complete on the M_{wg} scale than the M_w scale (Table 5).

Table 5. Difference in seismicity parameters between M_{wg} catalog and M_w catalog for different time periods.

	$\mathbf{M_{wg}}$	$\mathbf{M_w}$
M_c (1964–1990)	4.1 ± 0.17	4.7 ± 0.13
b	0.98	1.27
a	7.56	8.98
M_c (1964–2000)	4 ± 0.17	4.4 ± 0.17
b	0.85	0.95
a	6.86	7.57
M_c (1964–2012)	3.4 ± 0.11	4.1 ± 0.13
b	0.61	0.8
a	5.73	6.96
No. of Clusters	942 (22.381%)	1232 (31.882%)

Furthermore, the magnitudes of 'M_c', 'b,' and 'a' values for all the nine seismogenic zones have been determined. Only data on occurrences from 1964 to 2012 are used to calculate M_c values for distinct seismic zones, while the whole catalog for the period 1737–2012 is used for the estimate of 'b' and 'a' values. Table 6 displays the seismicity parameters for the various seismogenic zones.

Table 6. Estimated 'M_c', 'b,' and 'a' values for various seismogenic zones.

Seismogenic Zone	$\mathbf{M_c}$	'b'	'a'
I	3.4	0.6	5.02
II	3.5	0.66	5.51
III	3.9	0.7	4.96
IV	4.1	1.09	6.52
V	3.1	0.5	3.98
VI	3	0.45	3.84
VII	3.1	0.69	4.87
VIII	3.2	0.61	3.85
IX	3.3	0.65	4.92

7. Seismogenic Zones

The highest M_c value obtained is 4.1 for seismogenic zone IV, while the least M_c value found is 3 for seismogenic zone VI (Table 6). According to Table 6, the M_c value valid for the whole Northeast India area may be designated as 4.1 for the catalog term 1964–2012.

8. Discussion and Conclusions

A homogenous earthquake catalog is of critical importance to understanding the seismicity of a seismic region. A total of 9969 events during the period 1737–2012 for NE India have been considered in this study. As the M_w scale was mainly derived and validated for the Southern California region, therefore, a globally valid seismic moment magnitude scale M_{wg} is reported in recent literature. Improved GOR (GOR1) relationships for converting m_b and M_S to $M_{wg,GCMT}$ has been developed for the study region. For converting surface wave magnitudes to M_{wg} magnitudes, conversion relations have been developed for the ranges.

$4.1 \leq M_{s,ISC} \leq 6.1$ and $4.2 \leq M_{s,NEIC} \leq 6.1$, based on data 93 and 57 events, respectively. Similarly, Body wave magnitudes (m_b) are converted into M_{wg} scales following

the GOR1 methodology. The $m_{b,ISC}$ to $M_{wg,GCMT}$ conversion relationship has been developed using 116 event data for magnitude range $4.8 \leq m_{b,ISC} \leq 6.1$, while the $m_{b,NEIC}$ to $M_{wg,GCMT}$ conversion relationship is derived for magnitude range $4.8 \leq m_{b,NEIC} \leq 6.1$ based on 106 events.

A significant difference between M_w and M_{wg} estimations has been observed from various observed magnitudes such as m_b, M_S, M_L and M_D. Therefore, these differences in the seismic moment magnitude scales will lead to serious biased in the seismicity parameters and, consequently, in seismic hazard results (Table 5, [31]).

Only MMI intensity 5 and above data were utilized to construct an empirical relationship between intensity (I_{max}) and Seismic moment magnitude $M_{wg,GCMT}$. In total, 29 MMI intensities and $M_{wg,GCMT}$ data pairs are included from the entirety of India. The MMI empirical relationship for intensities 5 and higher is mostly compatible with the Indian seismic zoning chart, which shows the range of values associated with the major seismic zones according to the seismic code (IS, 2002) released by the Bureau of Indian Standards (BIS) [38]. Developed intensity-seismic moment magnitude relationship should be used to convert historical earthquakes to DMS (Das Magnitude Scale) scale when magnitude information is unavailable.

The declustering of the homogenized catalog for the time being 1737–2012 is carried out using the Ref. [36] procedure, and there is a reduction of 2231 events (22.38%) during this process. The entire homogenized earthquake catalog has been classified into four catalog periods, namely 1737–1963, 1964–1990, 1964–2000, and 1964–2012. For the four catalog periods, the magnitude of the completeness values is obtained using the EMR process. The M_c value declined from 5.6 for 1737–1964 to 3.9 for 1964–2012, as projected by a rise in instrumentation for this area beginning in 1964. Improving M_c has a major impact on the computation of the 'b' value and the assessment of the seismic hazard for a given location.

Several earthquakes of $M_{wg} \geq 7.0$ occurred in this area between 1737 and 2012. The maximum time elapsed between the occurrences of a major earthquake ($M_{wg} \geq 7.0$) was 18 years (1970–1988) in the 1737–2012 catalog. The last such occurrence happened in the area in 1988. The period of low seismic activity appears to have begun after 1988 and continues to this day.

The study area has been subdivided into nine seismogenic zones considering M_{wg} based earthquake catalogs, focal mechanisms, and fault types. 'M_c', 'b,' and 'a' values have been determined for each of these areas. The catalog data for the period 1897–2012 show that there have been no earthquakes of magnitude ≥ 7.0 in zones I, VI, or IX. Because zone IX is located between IV and VII zones in which big earthquakes have occurred, the probability of a big earthquake occurring in this zone is low in the immediate future. Based on these findings, a period of quiescence has been identified in seismogeneous zones I and VI for large-scale earthquakes.

A complete and consistent unified seismic catalog has been developed in terms of M_{wg} following a robust statistical procedure that could help to understand the seismicity of the region in a better way. Preparing a homogenized earthquake catalog by changing the original magnitude scales into seismic moment magnitude scale M_{wg}, an obstacle has been removed for seismic hazard assessment of the study region. Our analysis suggests that the use of the M_{wg} scale improves seismicity parameters 'b' up to 30%, 'a' up to 17%, and 'M_c' up to 38% for the Northeast India region (Table 5). Hence, the variations in these parameters may have a significant impact on the seismic hazard results. Therefore, the use of the M_{wg} scale is recommended for all practical cases.

Author Contributions: Conceptualization, R.D. and P.; data curation. R.D. and P.; formal analysis, R.D., P. and C.M.; investigation, R.D. and P.; methodology, R.D. and P.; resources, R.D.; software, R.D.; validation, R.D. and P.; visualization, R.D. and P.; writing—original draft, R.D., P., C.M., S.J. and T.B.; writing—review and editing, R.D., P., C.M., S.J. and T.B. All authors have read and agreed to the published version of the manuscript.

Funding: This research was supported by FONDECYT Grant 11200618.

Institutional Review Board Statement: Not applicable.

Informed Consent Statement: Not applicable.

Data Availability Statement: Body and surface wave magnitudes of earthquake data have been collected from ISC (International Seismological Center) U.K. (http://www.isc.ac.uk/search/Bulletin) (last accessed August 2012) and moment magnitudes have been collected from GCMT (Global Centroid Moment Tensor database, http://www.globalcmt.org/CMTsearch.html) (last accessed October 2012). Earthquake data of 9969 events for the time period 1897–2012 were compiled from various databases agencies (e.g. ISC, NEIC, GCMT, IMD, NEIST). Historical seismicity data were considered during 1897 to 1962 from Ref. [26].

Acknowledgments: We thank the Reviewers for their constructive comments, which largely improve the quality of this contribution.

Conflicts of Interest: The authors declare no conflict of interest.

Appendix A

Let M_x and M_y be the true values, and m_x and m_y be the derived values with δ and ε as magnitudes of errors in measuring for the independent and dependent variables. Then we can write:

$$m_x = M_x + \delta, \tag{A1}$$

$$m_y = M_y + \varepsilon, \tag{A2}$$

as well as the regression-like model:

$$m_y = \alpha + \beta M_x + \varepsilon, \tag{A3}$$

with $M_y = \alpha + \beta M_x$, where α and β are the slopes and intercepts of a linear relationship between genuine values

Mx, ε, and δ are assumed to be distributed in the relationships on a regular and independent basis.

The observed value covariances $\sigma^2_{m_y}$, $\sigma_{m_x m_y}$ and $\sigma^2_{m_x}$ are given by:

$$\sigma^2_{m_y} = \beta^2 \sigma^2_{M_x} + \sigma^2_{\varepsilon}, \tag{A4}$$

$$\sigma_{m_x m_y} = \beta \sigma^2_{M_x}, \tag{A5}$$

$$\sigma^2_{m_x} = \sigma^2_{M_x} + \sigma^2_{\delta}, \tag{A6}$$

where the error variance ratio:

$$\eta = \frac{\sigma^2_{\varepsilon}}{\sigma^2_{\delta}} \tag{A7}$$

If, $s^2_{m_y}$, $s^2_{m_x}$ and $s_{m_x m_y}$ are the sample covariances of m_y, m_x and between m_y and m_x, then:

$$s^2_{m_y} = \hat{\beta}^2 \hat{\sigma}^2_{M_x} + \eta \hat{\sigma}^2_{\delta}, \tag{A8}$$

$$s_{m_x m_y} = \hat{\beta} \hat{\sigma}^2_{M_x}, \tag{A9}$$

$$s^2_{m_x} = \hat{\sigma}^2_{M_x} + \hat{\sigma}^2_{\delta} \tag{A10}$$

The estimators $\hat{\beta}^2$, $\hat{\sigma}^2_{M_x}$ and $\hat{\sigma}^2_{\delta}$ maybe simply determined using the above simultaneous Equations (A8)–(A10). For example, the elimination of $\hat{\sigma}^2_{M_x}$ and $\hat{\sigma}^2_{\delta}$, we get the quadratic equation:

$$\hat{\beta}^2 s_{m_x m_y} - \hat{\beta}\left(s^2_{m_y} - \eta s^2_{m_x}\right) - \eta s_{m_x m_y}, \tag{A11}$$

Which yields

$$\hat{\beta} = \frac{s_{m_y}^2 - \eta s_{m_x}^2 + \sqrt{\left(s_{m_y}^2 - \eta s_{m_x}^2\right)^2 + 4\eta s_{m_x m_y}^2}}{2 s_{m_x m_y}} \tag{A12}$$

The $\hat{\sigma}_{M_x}^2$ and $\hat{\sigma}_{\delta}^2$ are similarly derived as follows:

$$\hat{\sigma}_{M_x}^2 = \frac{\sqrt{\left(s_{m_y}^2 - \eta s_{m_x}^2\right)^2 + 4\eta s_{m_x m_y}^2} - \left(s_{m_y}^2 - \eta s_{m_x}^2\right)}{2\eta}, \tag{A13}$$

$$\hat{\sigma}_{\delta}^2 = \frac{\left(s_{m_y}^2 + \eta s_{m_x}^2\right) - \sqrt{\left(s_{m_y}^2 - \eta s_{m_x}^2\right)^2 + 4\eta s_{m_x m_y}^2}}{2\eta} \tag{A14}$$

The estimator for α can be obtained from the relation:

$$\hat{\alpha} = \overline{m}_y - \hat{\beta}\overline{m}_x \tag{A15}$$

where $\overline{m}_x$ and $\overline{m}_y$ are the averages of the observed values.

Using Ref. [29] equations, the estimated variances of regression parameters $\hat{\beta}$ and $\hat{\alpha}$, may be expressed as follows:

$$\hat{\sigma}_{\hat{\beta}}^2 = \frac{\hat{\sigma}_{M_x}^2 (n-1)(\eta + \hat{\beta}^2)\hat{\sigma}_{\delta}^2 + \left(\hat{\sigma}_{\delta}^2\right)^2 (n-1)(\eta + \hat{\beta}^2) - (n-2)\left(-\hat{\beta}\hat{\sigma}_{\delta}^2\right)^2}{(n-2)(n-1)\left(\hat{\sigma}_{M_x}^2\right)^2} \tag{A16}$$

and

$$\hat{\sigma}_{\hat{\alpha}}^2 = \frac{(n-1)(\eta + \hat{\beta}^2)\hat{\sigma}_{\delta}^2}{n(n-2)} + \overline{m}_x^2 \hat{\sigma}_{\hat{\beta}}^2, \tag{A17}$$

where n is the sample size.

Appendix B. Descriptions of Various Notations Used in Our Study

Notation	Detail
$m_{b,ISC}$:	Body Wave Magnitude from ISC
$m_{b,NEIC}$:	Body Wave Magnitude from NEIC
$M_{S,ISC}$:	Surface Wave Magnitude from ISC
$M_{S,NEIC}$:	Surface Wave Magnitude from NEIC
$M_{L,IMD}$:	Local Magnitude from Indian Meteorological Department
M_L:	Local Magnitude Scale
$M_{D,NEIC}$:	Duration Magnitude from NEIC
M_0:	Seismic Moment
M_W:	Moment Magnitude was given by Ref. [8]
M_{wg}:	Seismic moment magnitude or Das magnitude Scale is given by Ref. [1]
$M_{wg,GCMT}$:	Seismic moment magnitude determined by GCMT
$M_{W,NEIC}$:	Moment Magnitude determined by NEIC
MMI:	Modified Mercalli Scale

GOR:	Conventional General Orthogonal Regression
GOR1:	General Orthogonal Regression gave by Ref. [19]
GOR2:	Conventional General Orthogonal Regression
SLR:	Standard Least square Regression
M_x:	Theoretical True value corresponding to the observed independent variable
M_y:	Theoretical True value corresponding to the observed dependent variable
η:	Error Variance Ratio
MSE:	Mean Square Error
MAE:	Mean Average Error
R_{xy}:	Correlation Coefficient
RMSE:	Root Mean Square Error

Appendix C. A Scheme for Conversions of Different Magnitude into $M_{wg,GCMT}$

Code 1: Proxy $M_{wg,GCMT}$ estimates from $M_{wg,GCMT}$ and $M_{S,NEIC}$
Code 2: Proxy $M_{wg,GCMT}$ estimates from $M_{wg,GCMT}$ and $M_{S,ISC}$
Code 3: Proxy $M_{wg,GCMT}$ estimates from $M_{wg,GCMT}$ and $M_{L,IMD}$
Code 4: Proxy $M_{wg,GCMT}$ estimates from $M_{wg,GCMT}$ and $m_{b,NEIC}$
Code 5: Proxy $M_{wg,GCMT}$ estimates from $M_{wg,GCMT}$ and $m_{b,ISC}$
Code 6: Proxy $M_{wg,GCMT}$ estimates from $M_{wg,GCMT}$ and $M_{D,NEIC}$
Code 7: Proxy $M_{wg,GCMT}$ estimates from $M_{wg,GCMT,}$ and M_S
Code 8: Proxy $M_{wg,GCMT}$ estimates from $M_{wg,GCMT}$ and $M_{W,NEIC}$

References

1. Das, R.; Sharma, M.; Choudhury, D.; Gonzalez, G. A Seismic Moment Magnitude Scale. *Bull. Seismol. Soc. Am.* **2019**, *109*, 1542–1555. [CrossRef]
2. Beresnev, I.A. The reality of scaling law of earthquake-source spectra? *J. Seismol.* **2009**, *13*, 433–436. [CrossRef]
3. Bormann, P.; Di Giacomo, D. The moment magnitude M_w and the energy magnitude M_e: Common roots and differences. *J. Seismol.* **2011**, *15*, 411–427. [CrossRef]
4. Bormann, P.; Saul, J. A Fast, Non-saturating Magnitude Estimator for Great Earthquakes. *Seismol. Res. Lett.* **2009**, *80*, 808–816. [CrossRef]
5. Das, R.; Meneses, C. A unified moment magnitude earthquake catalog for Northeast India. *Geomat. Nat. Hazards Risk* **2021**, *12*, 167–180. [CrossRef]
6. Choy, G.L.; Boatwright, J.L. Global patterns of radiated seismic energy and apparent stress. *J. Geophys. Res. Solid Earth* **1995**, *100*, 18205–18228. [CrossRef]
7. Choy, G.L.; Kirby, S.H. Apparent stress, fault maturity and seismic hazard for normal-fault earthquakes at subduction zones. *Geophys. J. Int.* **2004**, *159*, 991–1012. [CrossRef]
8. Hanks, T.C.; Kanamori, H. A moment magnitude scale. *J. Geophys. Res.* **1979**, *84*, 2348–2350. [CrossRef]
9. Ekström, G.; Dziewoński, A.M.; Maternovskaya, N.N.; Nettles, M. Global seismicity of 2003: Centroid–moment-tensor solutions for 1087 earthquakes. *Phys. Earth Planet. Inter.* **2005**, *148*, 327–351. [CrossRef]
10. Kanamori, H.; Anderson, D.L. Theoretical basis of some empirical relations in seismology. *Bull. Seismol. Soc. Am.* **1975**, *65*, 1073–1095.
11. Thingbaijam, K.K.S.; Nath, S.K.; Yadav, A.; Raj, A.; Walling, M.Y.; Mohanty, W.K. Recent seismicity in Northeast India and its adjoining region. *J. Seismol.* **2008**, *12*, 107–123. [CrossRef]
12. Ristau, J. Comparison of Magnitude Estimates for New Zealand Earthquakes: Moment Magnitude, Local Magnitude, and Teleseismic Body-Wave Magnitude. *Bull. Seismol. Soc. Am.* **2009**, *99*, 1841–1852. [CrossRef]
13. Das, R.; Wason, H.R.; Sharma, M.L. Magnitude conversion to unified moment magnitude using orthogonal regression relation. *J. Asian Earth Sci.* **2012**, *50*, 44–51. [CrossRef]
14. Das, R.; Wason, H.R.; Sharma, M.L. Homogenization of Earthquake Catalog for Northeast India and Adjoining Region. *Pure Appl. Geophys.* **2012**, *169*, 725–731. [CrossRef]
15. Das, R.; Wason, H.R.; Sharma, M.L. General Orthogonal Regression Relations between Body-Wave and Moment Magnitudes. *Seismol. Res. Lett.* **2013**, *84*, 219–224. [CrossRef]
16. Das, R.; Wason, H.R.; Sharma, M.L. Reply to 'Comment on "Magnitude conversion problem using general orthogonal regression" by H. R. Wason, Ranjit Das and M. L. Sharma' by Paolo Gasperini and Barbara Lolli. *Geophys. J. Int.* **2014**, *196*, 628–631. [CrossRef]

17. Das, R.; Wason, H.R.; Sharma, M.L. Unbiased Estimation of Moment Magnitude from Body- and Surface-Wave Magnitudes. *Bull. Seismol. Soc. Am.* **2014**, *104*, 1802–1811. [CrossRef]
18. Wason, H.R.; Das, R.; Sharma, M.L. Regression Relations for Magnitude Conversion for the Indian Region. In *Advances in Indian Earthquake Engineering and Seismology*; Sharma, M.L., Shrikhande, M., Wason, H.R., Eds.; Springer International Publishing: Cham, Switzerland, 2018; pp. 55–66. [CrossRef]
19. Das, R.; Wason, H.R.; Gonzalez, G.; Sharma, M.L.; Choudhury, D.; Lindholm, C.; Roy, N.; Salazar, P. Earthquake Magnitude Conversion Problem. *Bull. Seismol. Soc. Am.* **2018**, *108*, 1995–2007. [CrossRef]
20. Das, R.; Wason, H.R.; Sharma, M.L. Temporal and spatial variations in the magnitude of completeness for homogenized moment magnitude catalogue for northeast India. *J. Earth Syst. Sci.* **2012**, *121*, 19–28. [CrossRef]
21. Yadav, R.B.S.; Bormann, P.; Rastogi, B.K.; Das, M.V.; Chopra, S. A Homogeneous and Complete Earthquake Catalog for Northeast India and the Adjoining Region. *Seismol. Res. Lett.* **2009**, *80*, 609–627. [CrossRef]
22. Nath, S.K.; Mandal, S.; Das Adhikari, M.; Maiti, S.K. A unified earthquake catalogue for South Asia covering the period 1900–2014. *Nat. Hazards* **2017**, *85*, 1787–1810. [CrossRef]
23. Pandey, A.K.; Chingtham, P.; Roy, P.N.S. Homogeneous earthquake catalogue for Northeast region of India using robust statistical approaches. *Geomat. Nat. Hazards Risk* **2017**, *8*, 1477–1491. [CrossRef]
24. Anbazhagan, P.; Balakumar, A. Seismic magnitude conversion and its effect on seismic hazard analysis. *J. Seismol.* **2019**, *23*, 623–647. [CrossRef]
25. Dutta, T.K. Seismicity of Assam-zones of tectonic activity. *Seism. Assam Zones Tecton. Act.* **1964**, *2*, 152–163.
26. Gupta, H.K.; Rajendran, K.; Singh, H.N. Seismicity of Northeast India region: PART I: The database. *J. Geol. Soc. India* **1986**, *28*, 345–365.
27. Madansky, A. The fitting of straight lines when both variables are subject to error. *J. Am. Stat. Assoc.* **1959**, *54*, 173–205. [CrossRef]
28. Kendall, M.; Stuart, A. *The Advanced Theory of Statistics*; Griffin: London, UK, 1976; Volume 1, p. 102.
29. Fuller, W.A. *Measurement Error Models*; John Wiley & Sons: New York, NY, USA, 2009.
30. Carroll, R.J.; Ruppert, D. The use and misuse of orthogonal regression in linear errors-in-variables models. *Am. Stat.* **1996**, *50*, 1–6.
31. Vanzi, I.; Marano, G.C.; Monti, G.; Nuti, C. A synthetic formulation for the Italian seismic hazard and code implications for the seismic risk. *Soil Dyn. Earthq. Eng.* **2015**, *77*, 111–122. [CrossRef]
32. Contento, A.; Aloisio, A.; Xue, J.; Quaranta, G.; Briseghella, B.; Gardoni, P. Probabilistic axial capacity model for concrete-filled steel tubes accounting for load eccentricity and debonding. *Eng. Struct.* **2022**, *268*, 114730. [CrossRef]
33. Utsu, T. A method for determining the value of "b" in a formula log n = a-bM showing the magnitude-frequency relation for earthquakes. *Geophys. Bull. Hokkaido Univ.* **1965**, *13*, 99–103.
34. Gardner, J.K.; Knopoff, L. Is the sequence of earthquakes in Southern California, with aftershocks removed, Poissonian? *Bull. Seismol. Soc. Am.* **1974**, *64*, 1363–1367. [CrossRef]
35. Reasenberg, P. Second-order moment of central California seismicity, 1969–1982. *J. Geophys. Res. Solid Earth* **1985**, *90*, 5479–5495. [CrossRef]
36. Uhrhammer, R.A. Characteristics of northern and central California seismicity. *Earthq. Notes* **1986**, *57*, 21.
37. Wiemer, S. A software package to analyze seismicity: ZMAP. *Seismol. Res. Lett.* **2001**, *72*, 373–382. [CrossRef]
38. Standard, I. Criteria for earthquake resistant design of structures. *Bur. Indian Stand. Part* **1893**, *1*, 1–21.